

AD-A172 689

STRUCTURE OF THE EXTENDED EMISSION IN THE INFRARED  
CELESTIAL BACKGROUND(U) AIR FORCE GEOPHYSICS LAB  
HANSCOM AFB MA 5 D PRICE 30 SEP 86 AFGL-TR-86-0195

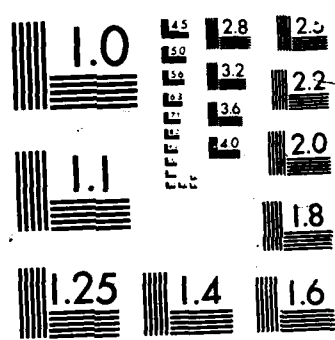
1/1

F/G 17/5

NL

UNCLASSIFIED





## AFGL-TR-86-0195

1

Structure of the Extended Emission in the Infrared Celestial Background

Stephan D. Price

Optical Physics Division, Air Force Geophysics Laboratory  
Hanscom AFB, MA 01731-5000Abstract

The extended emission in the infrared celestial background may be divided into three main components: the zodiacal background, the large discrete sources in the galaxy and the interstellar dust. The zodiacal background is due to the thermal re-radiation of sunlight absorbed by the dust in the solar system. An earth orbiting infrared telescope will detect the diffuse emission from this dust in all directions with maximum intensity lying roughly along the ecliptic plane where the density of dust is highest. Structure with scale lengths of  $10''$  have been measured in both the visual and infrared; finer structure has been detected in the infrared by the Infrared Astronomy Satellite (IRAS). H II regions, areas of ionized gas mixed with and surrounded by dust, are the brightest discrete objects in the galaxy in the long wavelength infrared (LWIR,  $7-30\mu\text{m}$ ). The visible radiation from the hot star(s) embedded in these regions is absorbed by the dust and re-emitted in the infrared with a range of temperatures characteristic of the thermal equilibrium for the surroundings of the dust. These regions are relatively large and, if close to the sun, can subtend a significant angular area of sky. The emission from the interstellar dust produces a filamentary structured background, the infrared "cirrus". The observed far infrared color temperature of  $\sim 20-35\text{K}$  for the cirrus is consistent with emission from graphite and silicate grains which absorb the interstellar radiation field. The much larger LWIR color temperature is likely due to a greater abundance of sub-micron particles in the interstellar medium and, perhaps, from band emission due to polycyclic aromatic hydrocarbons. These galactic sources combine along the line of sight to produce an intense band of emission centered on the galactic plane which has full width at half maxima of about  $2''$ .

Introduction

Meter class instruments such as the Infrared Space Observatory (ISO)<sup>1</sup>, an approved and funded project of the European Space Agency, and NASA's projected Space Infrared Telescope Facility (SIRTF)<sup>2</sup> are expected to have diffraction limited performance ( $<20\mu\text{r}$ ) in the LWIR at high sensitivity. Broad band photometry with these instruments is expected to have a sensitivity of  $400\text{ }\mu\text{Jy}$  ( $1\text{ Jy} = 10^{-26}\text{ W M}^{-2}\text{Hz}^{-1}$ ) or about  $10^{-21}\text{ W m}^{-2}\mu\text{m}^{-1}$  at  $11\mu\text{m}$  for a one second integration time characteristic of area surveys.

The system performance of such LWIR telescopes in near earth orbits will be limited by the general nature and detailed character of the natural background. Trade-offs between the detector size and sensitivity, the amount of data processing and the extent and location of avoidance regions are forced by the intensity and structure of the discrete and diffuse components in the background.

The ultimate sensitivity of any LWIR sensor is set by the photon flux on the detector from the diffuse zodiacal background. This emission is pervasive and is observable in all directions for a telescope in near earth orbit. However, the intensity is highly aspect dependent, being brightest near the sun and along the ecliptic plane where the density of the zodiacal dust is greatest. The large source densities and extended structure in the celestial background at the sensitivities projected for space borne infrared telescopes can create a confusion problem which can tax the data processing. The large scale infrared celestial emission, either nearby H II regions or the infrared "cirrus", is wispy in appearance with scale lengths ranging from many degrees down to at least as small as the  $0.22\mu\text{r}$  width of the IRAS detectors. The small scale structure can cause a clutter problem through jitter for a staring instrument such as a mosaic camera or directly for a scanning photometric measurement. The scan clutter problem is further compounded by registration difficulties due to field rotation.

The current observations on the extended celestial background is reviewed with emphasis on the LWIR. Some discussion of the physical processes involved and how they may be modeled is also included.

Zodiacal Emission

The zodiacal background is associated with dust in the solar system. The visual manifestation is due to reflected sunlight and is most prominently seen as an ellipsoidal glow in the twilight of the springtime setting sun or before sunrise in the fall. The infrared background arises from the thermal re-emission of the absorbed sunlight. The geometry of this phenomenon is related to that of the solar system and the pertinent quantities are defined below:

DTIC  
SELECTED  
OCT 06 1986  
S D

This document has been approved  
for public release and unlimited  
distribution is authorized.

UNCLASSIFIED

SECURITY CLASSIFICATION OF THIS PAGE

1172 609

## REPORT DOCUMENTATION PAGE

1a. REPORT SECURITY CLASSIFICATION <b>UNCLASSIFIED</b>		1b. RESTRICTIVE MARKINGS			
2a. SECURITY CLASSIFICATION AUTHORITY		3. DISTRIBUTION/AVAILABILITY OF REPORT Approved for public release Distribution unlimited			
2b. DECLASSIFICATION/DOWNGRADING SCHEDULE		4. PERFORMING ORGANIZATION REPORT NUMBER(S) <b>AFGL-TR-86-0195</b>			
5. MONITORING ORGANIZATION REPORT NUMBER(S)		6a. NAME OF PERFORMING ORGANIZATION <b>Air Force Geophysics Laboratory</b>			
6b. OFFICE SYMBOL (If applicable) <b>OPI</b>		7a. NAME OF MONITORING ORGANIZATION			
6c. ADDRESS (City, State, and ZIP Code) <b>Hanscom AFB Massachusetts, 01731</b>		7b. ADDRESS (City, State, and ZIP Code)			
8a. NAME OF FUNDING/SPONSORING ORGANIZATION		8b. OFFICE SYMBOL (If applicable)			
8c. ADDRESS (City, State, and ZIP Code)		9. PROCUREMENT INSTRUMENT IDENTIFICATION NUMBER			
		10. SOURCE OF FUNDING NUMBERS			
		PROGRAM ELEMENT NO. <b>62101F</b>	PROJECT NO. <b>7670</b>	TASK NO. <b>06</b>	WORK UNIT ACCESSION NO. <b>13</b>
11. TITLE (Include Security Classification) <b>Structure of the Extended Emission in the Infrared Celestial Background</b>					
12. PERSONAL AUTHOR(S) <b>Dr. Stephan D. Price</b>					
13a. TYPE OF REPORT <b>Reprint</b>	13b. TIME COVERED FROM _____ TO _____	14. DATE OF REPORT (Year, Month, Day) <b>1986 September 30</b>		15. PAGE COUNT <b>14</b>	
16. SUPPLEMENTARY NOTATION <b>SPIE Symposium ID #685-25      ESD Clearance #86-766 dated 29 August 1986</b>					
17. COSATI CODES		18. SUBJECT TERMS (Continue on reverse if necessary and identify by block number) <b>KEYWORDS: Infrared Background, Zodiacial Emission, HII Regions, Structured Emission</b>			
19. ABSTRACT (Continue on reverse if necessary and identify by block number) <b>The extended emission in the infrared celestial background may be divided into three main components: the zodiacial background, the large discrete sources in the galaxy and the inter-stellar dust. The zodiacial background is due to the thermal re-radiation of sunlight absorbed by the dust in the solar system. An earth orbiting infrared telescope will detect the diffuse emission from this dust in all directions with maximum intensity lying roughly along the ecliptic plane where the density of dust is highest. Structure with scale lengths of 10° have been measured in both the visual and infrared; finer structure has been detected in the infrared by the Infrared Astronomy Satellite (IRAS). H II regions, areas of ionized gas mixed with and surrounded by dust, are the brightest discrete objects in the galaxy in the long wavelength infrared (LWIR, 7-30 μm). The visible radiation from the hot star(s) embedded in these regions is absorbed by the dust and re-emitted in the infrared with a range of temperatures characteristic of the thermal equilibrium for the surroundings of the dust. These regions are relatively large and, if close to the sun, can subtend a significant (Cont'd)</b>					
20. DISTRIBUTION/AVAILABILITY OF ABSTRACT <input checked="" type="checkbox"/> UNCLASSIFIED/UNLIMITED <input type="checkbox"/> SAME AS RPT. <input type="checkbox"/> DTIC USERS			21. ABSTRACT SECURITY CLASSIFICATION <b>UNCLASSIFIED</b>		
22a. NAME OF RESPONSIBLE INDIVIDUAL <b>STEPHAN D. PRICE</b>			22b. TELEPHONE (Include Area Code) <b>(617) 377-4552</b>		22c. OFFICE SYMBOL <b>AFGL/OPI</b>

BLOCK 19. (Continued)

angular area of sky. The emission from the interstellar dust produces a filamentary structured background, the infrared "cirrus". The observed far infrared color temperature of ~20-35K for the cirrus is consistent with emission from graphite and silicate grains which absorb the interstellar radiation field. The much larger LWIR color temperature is likely due to a greater abundance of sub-micron particles in the interstellar medium and, perhaps, from band emission due to polycyclic aromatic hydrocarbons. These galactic sources combine along the line of sight to produce an intense band of emission centered on the galactic plane which has full width at half maxima of about 2°.

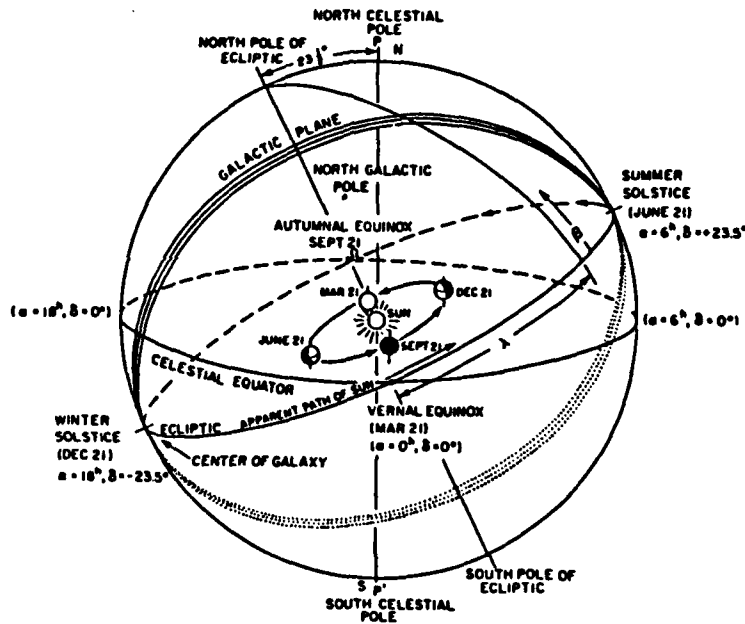


Figure 1. Co-ordinate Geometry.  $\delta$  is ecliptic longitude,  $\lambda$  is ecliptic latitude

- ecliptic plane
- ecliptic latitude ( $\lambda$ )
- ecliptic longitude ( $\delta$ )
- elongation (e)
- invariable plane
- astronomical unit (AU)
- albedo (a)

- the reflex of the earth's orbit on the sky
- angular measure perpendicular to the plane
- angular measure along the ecliptic plane from the vernal equinox (the intersection of the ecliptic plane and the celestial equator)
- angular measure from the sun
- the mean plane of the solar system defined as the angular momentum weighted average of all the orbital planes of the planets. The invariable plane is inclined 1.25° to the ecliptic with an ascending node (the point where a particle orbiting in the same direction as the planets would cross the ecliptic plane going from negative to positive latitude) of 107° longitude.
- the mean distance of the earth from the sun, about  $1.5 \times 10^8$  km.
- the ratio of reflected to incident energy of a particle

#### Visual Zodiacal Light

Until about a decade ago the majority of the data on the zodiacal background consisted of visual observations obtained by ground, balloon borne and satellite based platforms. Comprehensive reviews of these measurement are given by Leinert<sup>3</sup> and Weinberg and Sparrow<sup>4</sup>. Although the absolute intensities obtained by the various experiments show a high degree of internal consistency, they differ from one another by as much as a factor of two at large elongations in the ecliptic plane, a situation which exists even for recent observations. These discrepancies are likely due to systematic errors as Leinert et al<sup>5</sup> found that the visual zodiacal background inside the earth's orbit was constant, to within 2%, during a major portion of a solar cycle.

This constancy also places short term constraints on the dynamics of the dust. Wyatt and Whipple<sup>6</sup> have shown that a typical dust particle will spiral into the sun due to the Poynting-Robertson light drag in about  $10^4$  years. Constancy in the zodiacal light requires that at least  $10^6$  grams/sec of dust must be injected into the zodiacal cloud to balance the mass of dust sublimed by the sun or ejected from the solar system<sup>3</sup>. Estimates based on visual observations of the ejection rates of cometary dust and radio measurements on meteors account for only a small percentage of the required dust<sup>7</sup>. However, infrared observations indicate that these sources are more significant than implied by the visual data.

The plane of symmetry defined by the peak visual brightness lies neither in the ecliptic nor the invariable plane. Maucherat et al<sup>8</sup> derived a single plane for the zodiacal cloud at an inclination of 2° from an all sky survey taken by an earth orbiting satellite during a period of over a year. Other measurements<sup>9-11</sup> indicate that within .86 AU of the sun the peak brightness and, consequently, maximum dust density lies close to ( $i = 2.7^\circ$ ) but not in the orbital plane of Venus ( $i = 3.4^\circ$ ). Observations by Misconi<sup>11</sup> indicate that outside the orbit of Venus, the plane of symmetry tends to the invariable plane. Thus, the plane of maximum density of the dust in the zodiacal cloud, the symmetry plane, varies in inclination with respect to the ecliptic plane as a function of heliocentric distance.

The local volumetric absorption cross section of the dust can be derived by inverting the brightness

integral. If, as is generally assumed, the properties of the dust are independent of position then such an inversion traces the variation in particle density. Usually, the peak intensity of the zodiacal light is assumed to follow a power law ( $I \propto R^q$ ). Leinert et al<sup>12</sup> derived a value of  $q \sim -2.3$  inside the solar circle from observations with the Helios spacecraft. A steeper falloff ( $q \sim -2.6$ ) was found by Toller and Weinberg<sup>13</sup> between 1 and 2.4 AU from in situ measurements on board Pioneer 10 and 11. Inverting the brightness integral with the above assumptions results in a dust density proportional to  $R(q-1)$ . In a simple model, dust particles injected into the solar system from a single source acted upon by the Poynting-Robertson effect will have a  $1/R$  distribution<sup>6</sup>. The steeper falloff reported above ( $R^{-1.3}$  to  $R^{-1.6}$ ) implies that there are multiple sources distributed over an extended region<sup>14</sup> and/or focusing to the ecliptic plane due to collisions<sup>15</sup>. However, Schuemann<sup>16</sup> found that the brightness variation measured by Pioneer 10 was more complex than described by a single power law. Alternatively, Lamy and Perrin<sup>17</sup> adopt a  $1/R$  density distribution and explain the observed brightness variation in terms of an  $r^{-0.3}$  variation in the volume scattering function.

Out of the plane of symmetry, the observed visual brightness variations in ecliptic latitude for the region inside the earth's orbit are best represented by a modified fan shaped density distribution<sup>8,17,18</sup>.

In addition to the Gegenschein, enhanced back scattering of the dust particles at the anti-solar point, small scale structure has also been observed in the visible zodiacal light by Hong et al<sup>19</sup>. These local variations are reported to be about 10% in amplitude with a 7-10° scale length.

Infrared observations are complementary to the visual in constraining the characteristics of the dust and provide a better probe of the outer regions of the zodiacal clouds. The complex nature of the dust cloud as revealed by infrared observations is reviewed next.

#### Infrared Measurements

As a dust grain nears the sun its temperature rises until the sublimation point is reached. The grain sublimes, decreasing in size until the radiation pressure balances the Poynting-Robertson drag ( $d(\mu\text{m}) \propto (g \text{ cm}^{-3})^{-1}$ , Leinert<sup>3</sup>). If the grain temperature is independent of size, a local enhancement will be built up in the region where the grain temperature is near the vaporization point. Several regions of enhanced infrared emission near the sun were reported by ground and balloon based observations in the late 1960's 20-24, the most consistent is at 4 solar radii. A recent multi-color near infrared observations from a balloon platform<sup>25</sup> also detected a ring at 4 solar radii. The relative variation of the near infrared intensities as a function of solar distance are in good agreement between these experiments but the absolute values differ by as much as a factor of four. This discrepancy and the fact that the rings were not detected on all experiments led Koutchmy and Lamy<sup>26</sup> to speculate that the rings may be transitory. At longer wavelengths, several regions of enhanced emission were reported by Lena et al<sup>27</sup> at 10μm near the sun from an experiment flown on the Concorde during the 1973 total solar eclipse.

The near infrared observations of the zodiacal background at larger elongations are limited to two measurements near  $e \sim 25^\circ$  obtained on experiments flown in the early 1970's. Hayakawa et al<sup>28,29</sup> obtained multi-color near infrared measurements with a rocket borne experiment while Hofmann et al<sup>30</sup> used a balloon platform for measurements at 2.4μm. More extensive observations are needed on the near infrared zodiacal background as a function of position in order to map the transition from reflected sunlight to thermal emission.

Soifer et al<sup>31</sup> reported the first infrared observations of the thermal emission at larger elongations from the zodiacal dust with 5-6, 12-14 and 16-23μm photometry of a single plane crossing at  $e \sim 106^\circ$  from a sounding rocket. The results were rendered somewhat uncertain by the large contribution of off axis earth-shine to the measurement. The same group flew a subsequent spectrophotometric experiment<sup>32</sup> and obtained an 8-14μm spectrum of the emission peak from the plane at  $e \sim 103^\circ$ . The spectrum showed a broad silicate emission feature in excess of a 300K gray body continuum. This is consistent with recent laboratory measurements on captured interplanetary dust particles<sup>33</sup> which show prominent 10μm silicate features characteristic of chondritic material.

The largest data base on the LWIR emission from the zodiacal dust cloud is that obtained by the Optical Physics Division of the Air Force Geophysics Laboratory on a series of probe rocket borne experiments from 1974 to 1983 and by the Infrared Astronomy Satellite (IRAS) during 1983. The relative brightness at 11 and 20μm along the ecliptic between 35° and 75° elongation was measured on a September 1974 experiment<sup>34</sup>. These measurements have a systematic zero point error as they are relative to the brightness beyond  $|e| > 30^\circ$ , the region used as a zero reference in deconvolving the ac coupled signals. AFGL obtained LWIR spectrophotometry on several rocket flights. In 1975, several plane crossing were made between 3.5 and 26° elongation<sup>35</sup>. Later, more extensive coverage (22-85° and 137-180° elongation; from -60° ecliptic latitude to the north ecliptic pole) was obtained on the ZodiacaL Infrared Project (ZIP)<sup>36</sup>, a two flight experiment which sampled the zodiacal background in 15 spectral bands spanning the region from 2 to 30μm. A single plane crossing 19.5° from the sun was measured with a different set of filters during an October 1983 experiment.

IRAS observed the zodiacal emission between 60 and 120° elongation continuously over a 10 month period in 1983<sup>37</sup> in four broad spectral bands, 8-15, 16-30, 45-75 and 85-115μm. The survey aspect was restricted to within 30° of quadrature (the large majority of data lie in the region 75° < e < 105°) and the in plane brightness varied by only a factor of 4. On the other hand, the long period of observations with multiple rescans

of a given area covered all ecliptic longitudes with a range of viewing geometries.

Figure 2 compares the various brightnesses measured near  $11\mu\text{m}$  along the ecliptic plane. The IRAS data (circles) include the color correction of Hauser and Houck<sup>38</sup>. Spectral photometry at  $e \sim 22$  and  $90^\circ$  from various experiments is compared in figure 3. In general, the various measurements agree to within the quoted errors although there may be a trend for the IRAS in plane observations to be about 40% higher than the ZIP data. The agreement is much better at the pole as can be seen in figure 4. The AFGL experiments measured full width at half maxima (FWHM) of 7, 10 and  $70^\circ$  at  $e \sim 3.5, 22$  and  $90^\circ$ , respectively, which are nearly independent of wavelength over the spectral range of 6 to  $25\mu\text{m}$ . In contrast Hauser et al<sup>37</sup> report IRAS derived values at  $e \sim 90^\circ$  of  $83^\circ$  at  $12\mu\text{m}$  and  $68^\circ$  at  $25\mu\text{m}$ .

ECLIPTIC RADIANCE  
AS A FUNCTION OF  
ELONGATION  
ELONGATION 0. TO 180.  
ELEVATION 0.

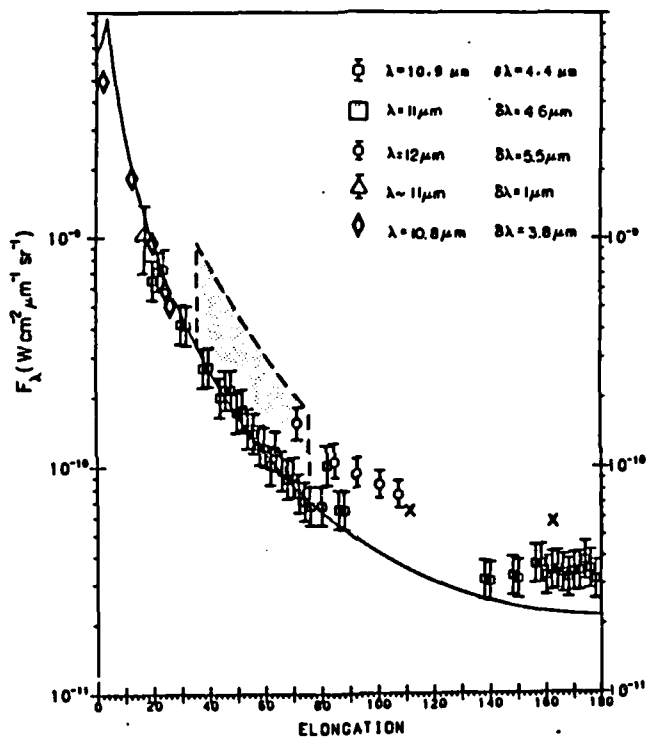


Figure 2. In Plane Variation of Zodiacal Brightness at  $11\mu\text{m}$ . The squares with error bars are the ZIP broad band  $11\mu\text{m}$  data<sup>36</sup>, crosses are from Soifer et al<sup>31</sup> and Briotta et al<sup>32</sup>, and the shaded area are the data of Price et al<sup>34</sup> corrected to the ZIP observations at  $|\beta| > 40^\circ$ . The circles represent the IRAS observations<sup>37</sup> with the corrections of Hauser and Houck<sup>38</sup>. The near sun measurements of Murdock<sup>35</sup> are shown by the diamonds and the unpublished 1983 rocket borne measurement at  $e \sim 22^\circ$  is the triangle with the estimated error. The reference line is the simple model described by Murdock and Price<sup>36</sup> with a  $1/R$  density distribution.

The reference curves in figures 2-4 are from the simple model formulated by Price and Murdock<sup>35</sup> which adopts a mean particle size, albedo and a fan shaped density distribution with a  $1/R$  in plane variation and provides a reasonable fit to the observations. A more rigorous model by Frazier et al<sup>39</sup> assumes a  $1/R$  density variation, a three regime power law distribution of particle sizes and albedos derived from the optical constants of the adopted chemical composition of the material and Mie scattering theory. Although there is reasonable agreement between this model and the in plane visual intensity and the polarization, the infrared values are discordant by at least a factor of two at the anti solar point. Thus the infrared properties of the dust are not simple functions of solar distance<sup>35</sup>. By inverting the brightness integral for the ZIP observations, Hong and Um<sup>40</sup> deduce that, indeed, the density of the dust varies markedly with solar distance. They further concluded that the infrared properties of the dust are not spatially homogeneous and that the visual observations sample a different mixture of dust properties than the infrared. Of course, such conclusions depend on the model assumptions. For instance, Dumont and Levasseur-Regourd<sup>41</sup> interpret the variation of dust properties as due to a change in albedo. They derived values of  $a = .08$  at .98 AU and .06 at 1.4 AU from IRAS measurements and propose that the steeper  $R^{-2.3}$  falloff found in the

visual represents a shallower density variation ( $1/R$  in agreement with the infrared data) coupled with a albedo which decreases with heliocentric distance.

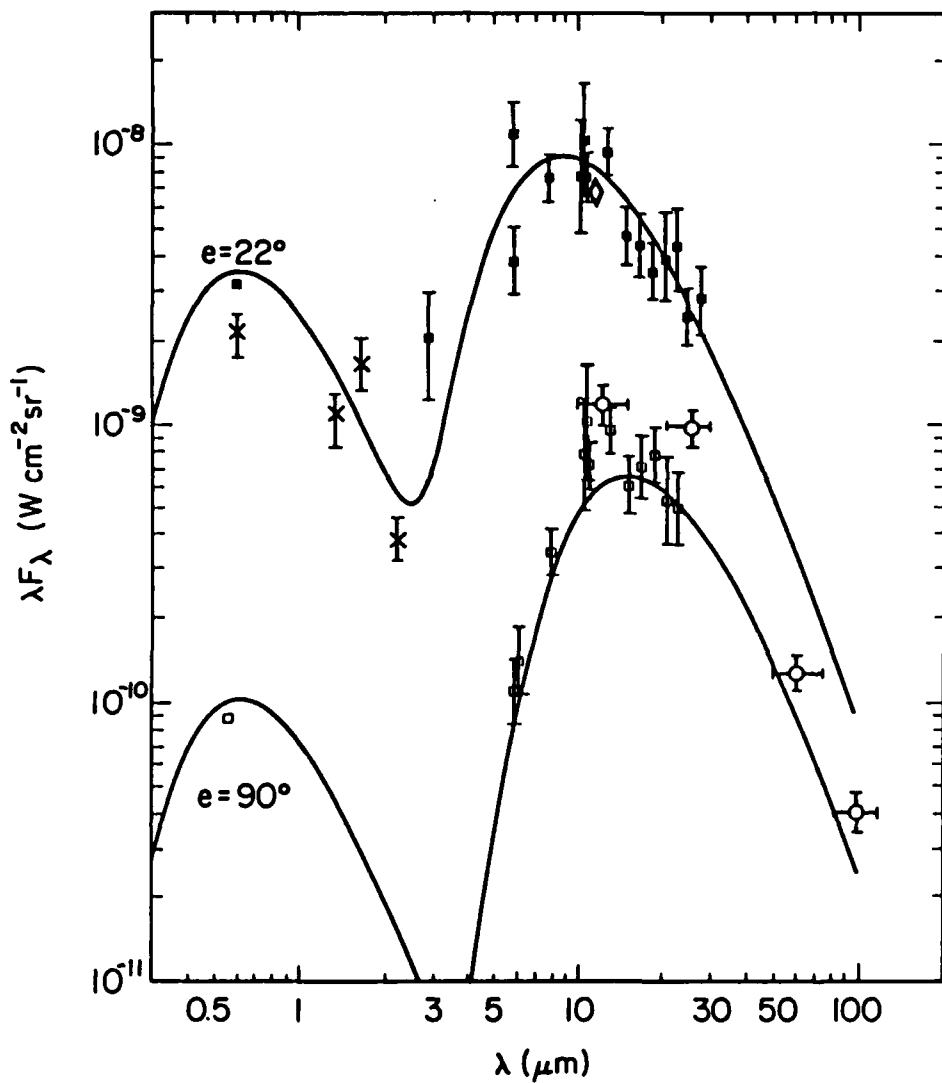


Figure 3. In Plane Spectra of Zodiacal Emission. Squares, circles and the diamond have the same designations as in Figure 1 (the visual points are taken from Allen's "Astrophysical Quantities"). The crosses are observations analyzed by Nishimura<sup>29</sup>.

The plane of symmetry of the zodiacal dust cloud defined by the peak infrared emission lies neither in the ecliptic nor invariable planes, in qualitative agreement with visual measurements. The recent results based on IRAS data for the geometry of the cloud as reviewed by Hauser et al<sup>42</sup> have an inclination of 2-2.5° and an ascending node of 74-78° for the plane near 1 AU from the seasonal variation of the brightness at the ecliptic poles and a 1.5° inclination with a 55° ascending node for the material outside the orbit of the earth based on the longitudinal dependence of the latitude of the peak emission. From an analysis of the IRAS 25 μm observations of the peak brightness and the latitude variation with longitude, Dermott et al<sup>43</sup> concluded that the plane of symmetry is either warped or that the infrared zodiacal dust cloud is not axisymmetric. The peak 25 μm brightness was well fit by a parabolic variation in elongation.

Also on the global scale, IRAS detected<sup>45</sup> bands of enhanced zodiacal emission centered on the plane of symmetry and 10° either side of it. The 2.2-2.3 AU solar distance of the bands was inferred by their 165-200K color temperature was subsequently supported by photometric parallax measurements of the separation of the bands as a function of elongation<sup>46</sup>. Dermott et al<sup>43,47</sup> have argued that these bands are the geometric projections of dust and small particles associated with the prominent Hirayama asteroid families, Eos and Themis. Sykes and Greenberg<sup>48</sup> calculated that a single collision several million years ago between two members of these families some 15-25km in diameter could produce the band as seen today. Further, given a reasonable asteroidal size distribution and collision rate in the Hirayama families as many as 20 more bands may be detectable in the IRAS data; the more recent events would form arcs rather than complete

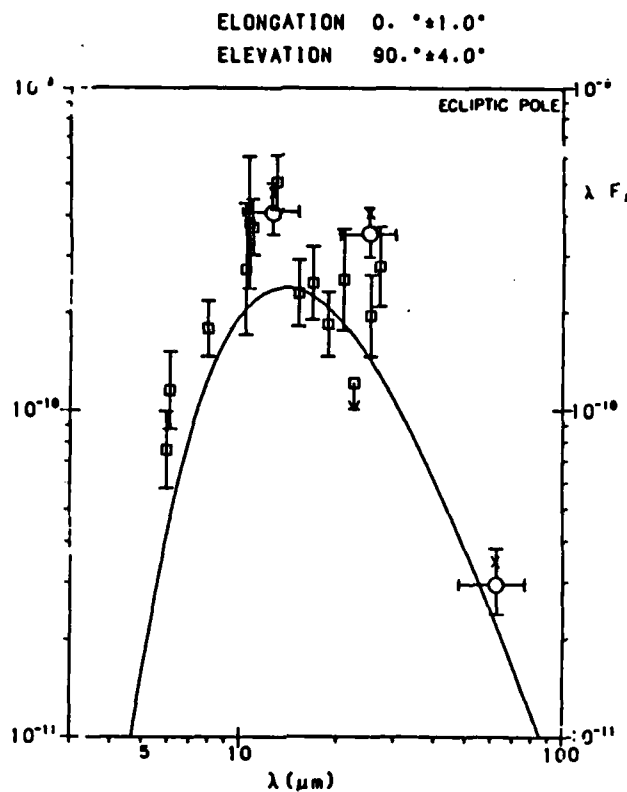


Figure 4. Zodiacal Spectrum at the Ecliptic Pole. Comparison of the ZIP (squares) and IRAS (circles) observations at the north ecliptic pole.

bands. The small debris from such an event would collide with the background zodiacal dust resulting in further fragmentation. Collision fragments are removed from the bands to become part of the general background of zodiacal dust when the Poynting-Robertson drag on the resulting particles exceeds about 10 times the gravitational force. Sykes and Greenberg<sup>48</sup> conclude that the majority of the zodiacal dust is produced in this manner.

The IRAS Asteroid Data Analysis System is analyzing several million sources with solar system colors which were detected on a single orbit but not confirmed on a subsequent scan (that is, a potential moving object). Over 10,000 of these observations have been associated with numbered asteroids<sup>49</sup>. Unassociated, high quality observations (in two or more spectral bands with proper color temperature) in this file show a marked concentration to the ecliptic plane<sup>50</sup> which argues that the file probably contains numerous measurements of small asteroids or comets. Dust strewn along the orbit of short period comets should also be an important contributor to this file. For instance, the dust trail from P/Temple 2 was found in the IRAS data by Davies et al<sup>51</sup> as 50 faint seconds confirmed sources detected in July of the IRAS emission and subsequently confirmed on rescanning.

A study of the large scale IRAS sky flux maps by Sykes et al<sup>52</sup> turned up numerous dust trails and streaks in the zodiacal background. In addition to P/Temple 2, dust trains from P/Enke, P/Gunn and P/Schwassmann-Wachmann I have been positively identified. P/Temple 2 has the brightest trail and was detected over at least  $48^{\circ}$  of the sky, which corresponds to over 1 AU in length. Sykes<sup>53</sup> resolved the comet and tail in an IRAS coadded map and was able to distinguish the dust trail from the large particle component of the tail. Thus, cometary ejecta have a bimodal distribution; a small component sensitive to radiation pressure and a millimeter/centimeter component which remains in the orbit of the comet. The amount of material distributed along the detectable length of the P/Temple 2 trail is estimated at about  $10^{12}$  grams<sup>52</sup> to over  $10^{10}$  kg<sup>53</sup>. This dust was deposited over a period of several hundreds of years by numerous emission events. This is the same order of magnitude as the 5,000 ton mass ejection per perihelion passage estimated by Singer et al<sup>55</sup> for the Enke stream. Sykes et al also found evidence of at least 100 other trails in the sky flux maps but have been able to only tentatively associate trails with P/Temple 1, P/Kopff and P/Shoemaker 2. These trails are generally narrow, only a few of the 2' pixels in the sky flux maps, and most are less than a few degrees in length. The trails vary in brightness, length as ecliptic position. The most distant comet with a dust trail is P/Schwassmann-Wachmann I which was observed at 6.3 AU from the sun.

At 100 to 1000 times the sensitivity of the IRAS survey, future space borne telescopes will have to observe against a structured zodiacal background. The bands, arcs, dust trails, asteroids and comets which

populate the IRAS data base will be prominent LWIR objects at these intensity levels.

#### Extended Galactic Background

The extended LWIR galactic background is primarily due to emission from dust. Galactic gas and dust are concentrated to the galactic plane with a thickness of about 200 pc (pc = 202625 AU =  $3.09 \times 10^{18}$  cm) inside the solar circle and increasing height with galactocentric distance beyond the sun. About  $3 \times 10^9$  solar masses ( $M_{\odot} = 2 \times 10^{33}$  grams) of the gas is neutral atomic hydrogen (HI) which is more or less evenly divided between cloud and intercloud material<sup>56</sup>. An equal, or slightly greater, mass of gas is molecular, predominantly molecular hydrogen. Dust comprises only about 1% of the mass of the interstellar material, which itself is less than 10% of the total mass of the galaxy.

Most of the molecular gas is contained to the 6000-plus giant molecular clouds (GMC's) which lie along the spiral arms<sup>57</sup>; the rest is in the numerous smaller clouds distributed throughout the galaxy. The GMC's are massive,  $5 \times 10^4 - 10^6 M_{\odot}$ , gravitational bound objects with an average diameter of 40 pc<sup>58</sup>. About three quarters of the clouds larger than 20 pc in diameter have low kinetic temperature ( $\sim 10$ K) characteristic of an optically thick cloud in the interstellar environment. The remaining clouds have internal sources of heating due to recently formed stars and are closely associated with H II regions<sup>59</sup>. These molecular clouds generally exhibit a considerable degree of internal structure with extensive fragmentation, numerous condensations and filamentary structures.

H II regions are created around a newly formed O or B star ( $T_{\text{eff}} > 15,000$ K) or cluster of stars. The stellar uv flux completely ionizes the surrounding hydrogen (hence the designation H II, I represents the neutral ion - II singly ionized, etc. ), helium is singly ionized and most of the other elements are either singly or doubly ionized. The ionized electrons are collisionally thermalized and the nebula is cooled and the kinetic temperature is stabilized to about 10,000K by forbidden line emission from the recombination of electrons and ions. The line intensities are large and the H II region is visible over considerably distance. Indeed, these regions are used to estimate extra-galactic distances.

H II regions are prodigious infrared emitters. The majority of the visual and uv flux from the embedded star(s) is absorbed by the dust surrounding the H II region and then is thermally re-emitted in the infrared. The flux from a typical H II region generally peaks at about 70 $\mu\text{m}$  but the spectral energy distribution is much broader than blackbody emission at a single temperature with significant LWIR emission. Harris and Rowan-Robinson<sup>60</sup> estimated the core brightness of a typical large H II region at  $10^{10} \text{ w cm}^{-2} \mu\text{m}^{-1}$  at 10 and 20  $\mu\text{m}$ .

The large size and infrared luminosity of these regions make them easily detectable throughout the galaxy. The closer regions are easily resolved at moderate resolution ( $< 1\text{mr}$ ) and can cover a large area of sky; the Orion complex spans over 100 square degrees in area.

The most pervasive large scale background is the infrared cirrus. This highly structured emission is detectable over the entire sky and is indistinguishable in appearance from the filaments in the outer regions of H II regions and molecular clouds. Gautier<sup>61</sup> described the appearance of the cirrus as having "long, spider-like filaments, clumps and long arching structures composed of small wisps, filaments and clumps. Small scale structure is seen down to the resolution of the IRAS data, 2 to 4 arc minutes". The complex structure of the infrared cirrus, molecular clouds and H II regions can present a aspect dependent clutter problem for an area survey with a meter class telescope which can either increase noise or result in spurious sources. The magnitude of the problem depends on the intensity of the filamentary structure at the resolution of the instrument. Armstrong et al<sup>62</sup> determined that electron density fluctuations in the interstellar medium has a density spectrum of the form (size)  $3.6 \pm 0.2$ , consistent with a Kolmogorov spectrum (exponent = 11/3) for the energy cascade to smaller sizes due to turbulence. Such a steep function would predict little energy in microfilaments at the resolution of a meter class infrared telescope. The recent measurements on the turbulent spectra of molecular clouds<sup>63</sup> and H II regions<sup>64</sup> indicate a shallower power function than due to Kolmogorov processes. These observations indicate that the interstellar medium is compressible or that there are additional sources of energy at smaller scales.

Gautier<sup>61</sup> noted the correlation between the infrared cirrus and the high latitude reflection nebula studied by Sandage<sup>65</sup> which indicates that some significant fraction of the cirrus is near the sun ( $\sim 100$ pc) and that the dust re-emits the absorbed integrated star light from the galactic plane. A more quantitative study by DeVries and LePoole<sup>66</sup> found that the 100 $\mu\text{m}$  cirrus emission correlated well with visual extinction (the amount of dust) derived from star counts for two high latitude reflection nebula and that the infrared temperature of the clouds were extremely constant indicating that starlight, rather than an internal source powered the infrared emission. Sandage's description of the two faint reflection nebula he studied is quite similar to that of Gautier for the infrared cirrus. Sandage noted that one cloud was finely filamented on a scale as small as 30" which indicates that significant cirrus emission is likely to be present on comparable scales.

Correlation has also been found between the infrared cirrus, HI emission<sup>67</sup> and molecular clouds (CO emission)<sup>68</sup>. This was not too surprising since it has been known for some time that interstellar dust, as detected through visual extinction of starlight, is well correlated with the column density of gas (HI plus molecules)<sup>69</sup>. The 20-30K color temperatures of the infrared cirrus derived from the 60 to 100  $\mu\text{m}$  IRAS observations is consistent with heating by the interstellar radiation field; although Harwit et al<sup>70</sup> have

argued that a significant portion of the cirrus emission in these bands are due to forbidden line emission from [O I] and [O III]. The large amount of LWIR emission (IRAS 12 and 25 $\mu$ m bands)<sup>67,71</sup> was however, unexpected. Not only is the LWIR emission orders of magnitude larger than expected on the basis of the long wavelength observations but the 12 $\mu$ m:25 $\mu$ m color temperatures are also high (> 300K).

Part of this emission is probably due to the non-equilibrium heating of small dust grains by the uv in the interstellar radiation field. Draine and Anderson<sup>72</sup> calculated that substantial amounts of continuum radiation at less than 50 $\mu$ m can result in temperature fluctuations in small interstellar graphite and silicate grains. These temperature fluctuations are large when the energy of the absorbed photon is comparable, or greater, than the average heat content of the grain. For the interstellar radiation field this will occur for grains with radii < .01 $\mu$ m. This was found to account for some, but not all, the LWIR excess on a galactic scale<sup>73</sup>.

Puget et al<sup>74</sup> suggest that a significant fraction of the interstellar LWIR radiation is due to band emission from polycyclic aromatic hydrocarbons (PAH's). Leger and Puget<sup>75</sup> noted the similarity in the laboratory spectrum of the PAH molecule Coronene and the unidentified emission features at 3.3, 3.4, 6.2, 7.7, 8.6 and 11.3  $\mu$ m in reflection nebula and some H II regions. PAH's have not yet been observed in the cool interstellar medium although Leger and d'Hendecourt<sup>76</sup> and Crawford et al<sup>77</sup> find a reasonable match between the absorption spectrum of singly ionized PAH's and the diffuse interstellar bands in the visual. On the basis of this investigation Leger and d'Hendecourt conclude that only a small number PAH's are stable in the interstellar medium but that they are the most abundant molecules after H<sub>2</sub> and CO. Duley and Williams<sup>78</sup> on the other hand, claim that PAH's exist only in regions of shock formation since chemical reactions with H and O will effectively destroy them in the interstellar clouds. Instead, hydrogenated amorphous carbon dust will form in denser diffuse clouds and dark clouds. This could, in part, account for the variation of the 12 to 100 $\mu$ m intensity ratio from cloud to cloud and different regions of infrared cirrus.

The overlapping of the emission from the infrared cirrus, discrete and extended sources along the line of sight and in the sensor field of view results in an intense diffuse LWIR emission centered on the galactic plane, a portion of which is shown in figure 5. The emission is nearly constant out to 60° of either side of the center with a nearly exponential decrease at larger longitudes. The 2.4 and 4 $\mu$ m background<sup>79</sup> can be accounted for by stellar sources reddened by interstellar extinction. The emission in the far infrared can be attributed to dust in the galactic plane heated either by the interstellar radiation field or hot O and B stars<sup>73</sup>. The LWIR emission along the galactic ridge is again in excess of predictions. If the observed 10 $\mu$ m emission is accounted for by adding circumstellar dust shell sources to the point source model that adequately describes the near infrared background, the ridge brightnesses at 20 and 27 $\mu$ m are overpredicted. If, as suggested by Cox et al<sup>73</sup>, a significant portion of the LWIR emission from the galactic plane is from PAH's then their characteristic band features may be observable. Spectrophotometry of the diffuse emission from the galactic plane at a longitude of 36° in figure 6 along with the star burst galaxy M82, for comparison, which has strong PAH band emission. The 375K grey body spectral distribution is characteristic of the 4 $\mu$ m:11 $\mu$ m:20 $\mu$ m color temperature of the emission<sup>80</sup> is shown. The spatial (5'x15') and spectral (1-4 $\mu$ m) resolutions of the measurement is too coarse for unambiguous interpretation. However, the spectrum is consistent with emission bands from dust at 7.7+8.6 $\mu$ m and 11.3 $\mu$ m in addition to a silicate absorption.

#### Conclusion

Extended celestial emission will present a complex and varied background for a spaced based, cryogenic LWIR telescope system. Dust arcs, comet trails and asteroids in the solar system provide (moving) sources of spurious signals for area surveys. The highly structured and filigreed background due to structure in molecular clouds, H II regions and infrared cirrus could be a source of scan noise and spurious signals due to field rotation and scan aspect. Evidence indicates that this structure is present down to the resolutions of a meter class instrument and thus cannot be avoided with small fields of view. Strong arguments exists, including a low resolution spectrum of the diffuse emission from the galactic plane, that emission from this background has a great deal of spectral structure.

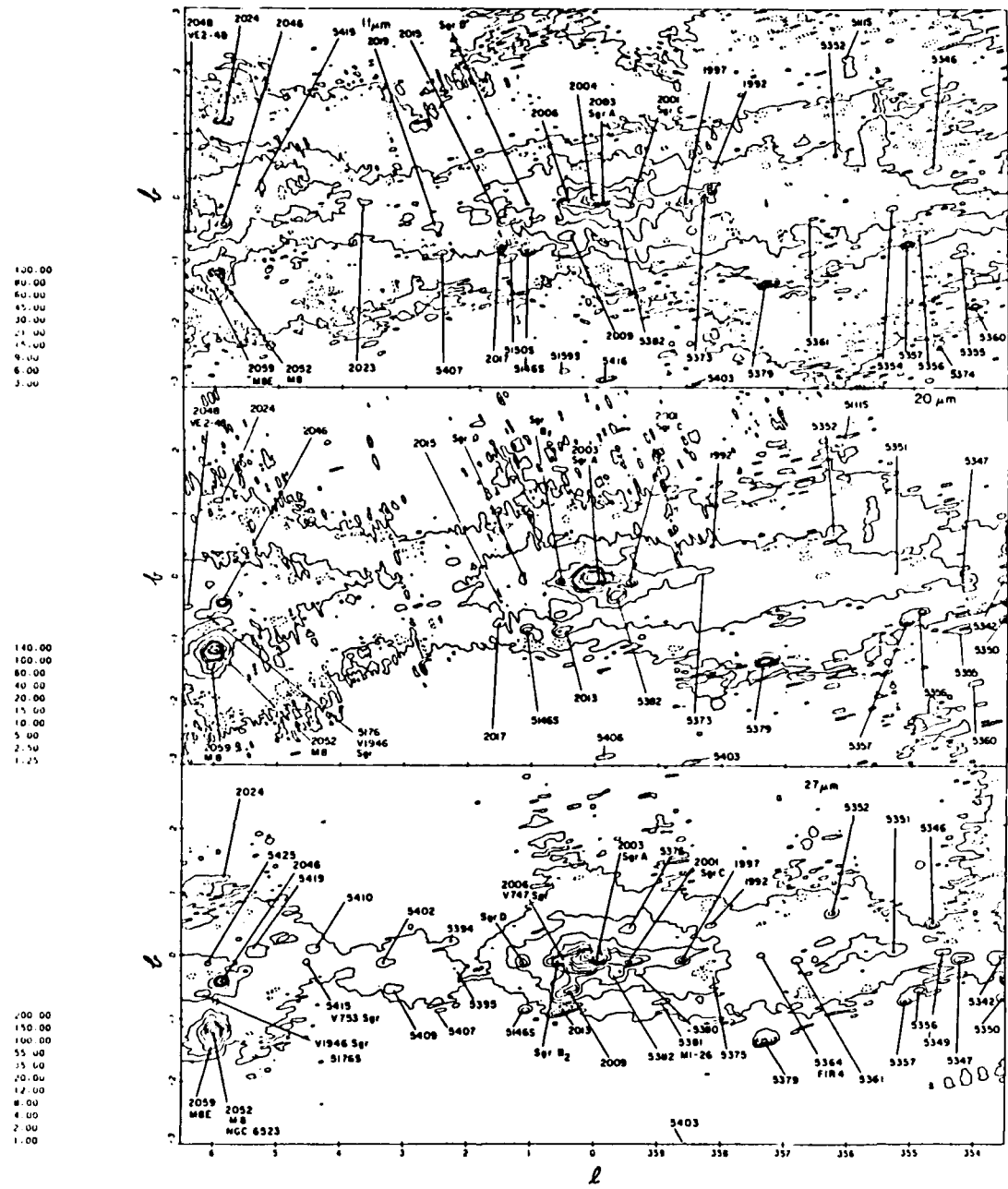


Figure 5. The Diffuse Emission Near the Galactic Center. The 11, 20 and 27  $\mu$ m maps of the diffuse emission near the galactic center. The discrete sources are identified, the unlabeled numbers refer to the AFGL catalog. Contour levels are in units of  $10^{-11} \text{ w cm}^{-2} \mu\text{m}^{-1} \text{ sr}^{-1}$ .

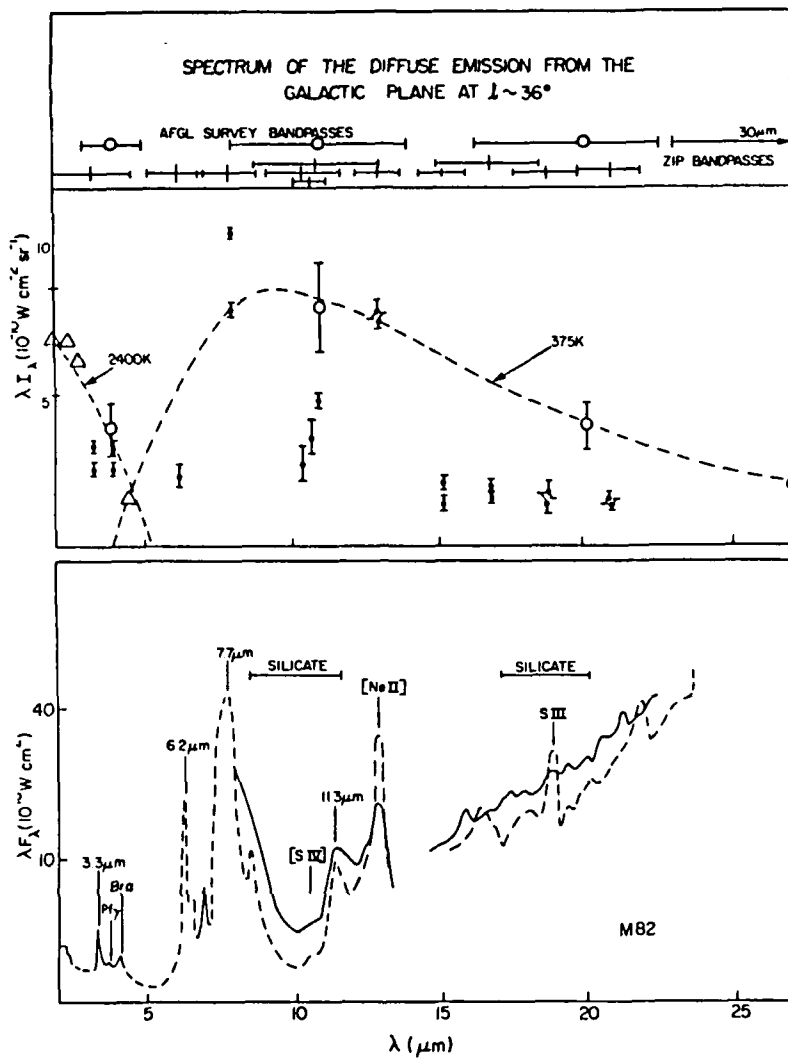


Figure 6. Spectrophotometry of the Galactic Plane. Triangles are balloon<sup>80</sup> and rocket borne<sup>81</sup> near infrared measurements, the open circles are from the AFGL survey<sup>80</sup> and squares the ZIP observations. Error bars are estimated internal errors. ZIP observations at the same wavelength are from separate detectors and are shown individually since the detectors track slightly different regions of the plane. The respective bandwidths of the observations are depicted at the top. The dusty galaxy M82 is shown for comparison of the spectral features. IRAS low resolution spectral data is the solid line at  $\lambda > 8\mu\text{m}$ . The dashed line is higher resolution data of the central 28" from Willner et al<sup>82</sup> and Houck et al<sup>83</sup> which have been scaled by a factor of two to match the IRAS data. The emission features in M82 have been identified.

#### References

1. "Infrared Space Observatory", ESA Report Phase A Study, Nov. 1982, (page) t SCI (82) 6, 1982.
2. Rieke, G.H., M.W. Werner, R.I. Thompson, E.E. Becklin, W.F. Hoffmann, J.R. Houck, F.J. Low, W.A. Stein and F.C. Witteborn, "Infrared Astronomy after IRAS", Science, Vol. 231, 807, 1986.
3. Leinert, C., "Zodiacal Light - A Measure of the Interplanetary Environment", Space Sci. Rev., Vol 18, 281, 1975.
4. Weinberg, J.L. and J.G. Sparrow, "Zodiacal Light as an Indicator of the Interplanetary Dust", Cosmic Dust, ed J.A.M. McDonnell, Wiley and Sons, 55, 1975.
5. Leinert, C., I. Richter and B. Planck, "Stability of Zodiacal Light from Minimum to Maximum of the Solar Cycle (1974-1982)", Astron. Astrophys., Vol. 110, 111, 1982.

6. Wyatt Jr., S.P., and F.L. Whipple, "The Poynting-Robertson Effect on Meteor Orbits", Astrophys. J., Vol. 111, 134, 1950.
7. Kresak, L., "Source of Interplanetary Dust", IAU Symp. 90: Solid Particles in the Solar System, D. Reidel, 211, 1980.
8. Maucherat, A., A. Llebaria, J.C. Gonin., "Zodiacal Light, Gegenschein and Sky Background", IAU Colloq. 85: Properties and Interactions of Interplanetary Dust, D. Reidel, 27, 1985.
9. Leinert, C., M. Hanner, I. Richter and E. Pitz, "The Plane of Symmetry of the Interplanetary Dust", Astron. Astrophys., Vol. 82, 328, 1980.
10. Nikolsky, G., S. Koutchmy, P.L. Lamy and I.A. Nesmjanovich, "Photographic Observations of the Inner Zodiacal Light Aboard Salyout 7", IAU Colloq. 85: Properties and Interactions of Interplanetary Dust, D. Reidel, 7, 1985.
11. Misconi, N.Y., "The Symmetry Plane of the Zodiacal Cloud near 1 AU", IAU Symp. 90: Solid Particles in the Solar System, 49, 1980.
12. Leinert, C., I. Richter, E. Pitz and B. Planck, "The Zodiacal Light from 1.0 to .3 AU as Observed by the Helios Space Probes", Astron. Astrophys., Vol. 103, 177, 1981.
13. Toller, G.N. and J.L. Weinberg, "The Change in Near-Ecliptic Zodiacal Light with Heliocentric Distance", IAU Colloq. 85: Properties and Interactions of Interplanetary Dust, D. Reidel, 21, 1985.
14. Leinert, C., "Dynamics and Spatial Distribution of Interplanetary Dust", IAU Colloq. 85: Properties and Interactions of Interplanetary Dust, D. Reidel, 369, 1985.
15. Trulsen, J. and A. Wiken, "Poynting-Robertson Effect and Collisions in the Interplanetary Dust Cloud", IAU Symposium 90: Solid Particles in the Solar System, D. Reidel, 299, 1980.
16. Schuerman, D.W., "Evidence that the Properties of Interplanetary Dust Beyond 1 AU are Not Homogeneous", IAU Symp. 90: Solid Particles in the Solar System, D. Reidel, 71, 1980.
17. Lamy, P.L. and J.-M. Perrin, "Volume scattering function and space distribution of the interplanetary dust cloud", Astron. Astrophys., Vol. 163, 269, 1986.
18. Giese, R.H., G. Kinateder, B. Kneissel and U. Rittich, "Optical Models of the Three Dimensional Distribution of Interplanetary Dust", IAU Colloq. 85: Properties and Interactions of Interplanetary Dust, D. Reidel, 255, 1985.
19. Hong, S.S., N.Y. Misconi, M.H.H. van Dyke, J.L. Weinberg and G.N. Tollner, "A Search for Small Scale Structure in the Zodiacal Light", IAU Colloq. 85: Properties and Interactions of Interplanetary Dust, D. Reidel, 33, 1985.
20. Peterson, A.W., "Experimental Detection of Thermal Radiation from Interplanetary Dust", Astrophys. J. (Letters), Vol. 148, L37, 1967.
21. Peterson, A.W., "The Coronal Brightness at 2.23 Microns", Astrophys. J., Vol. 155, 1009, 1969.
22. Peterson, A.W., "A Determination of the Vaporization Temperature of Circumsolar Dust at  $4R_O$ ", Bull. Amer. Ast. Soc., Vol. 3, 500, 1971.
23. MacQueen, R.M., "Infrared Observations of the Outer Solar Corona", Astrophys. J., Vol. 154, 1059, 1968.
24. Mankin, W.G., R.M. MacQueen and R.H. Lee, "The Coronal Radiance in the Intermediate Infrared", Astron. Astrophys., Vol 31, 17, 1974.
25. Maihara, T., K. Mizutani, N. Hiramoto, H. Takami and H. Hasegawa, "A Balloon Observation of the Thermal Radiation from the Circumsolar Dust Cloud in the 1983 Total Eclipse", IAU Colloq. 85: Properties and Interactions of Interplanetary Dust, D. Reidel, 55, 1985.
26. Koutchmy, S., and P.L. Lamy, "The F-Corona and Circum-Solar Dust Evidences and Properties", IAU Colloq. 85: Properties and Interactions of Interplanetary Dust, D. Reidel, 63, 1985.
27. Lena P., Y. Viala, D. Hall and A. Scufflet, "The Thermal Emission of the Dust Coronal During the Eclipse of June 30, 1973 II. Photometric and Spectral Observations", Astron. Astrophys., Vol. 37, 81, 1974.
28. Hayakawa, S., T. Matsumoto and T. Nishimura, "Infrared Observations of the Zodiacal Light", Space Research Vol X, 249, 1970.

29. Nishimura, T., "Infrared Spectrum of Zodiacal Light", Publ. Astron. Soc. Jap., Vol. 25, 375, 1973.

30. Hofmann, W.D., D. Lemke, C.D. Thum and U. Fahrback, "Observations of the Zodiacal Light at 2.4  $\mu$ m", Nature Phys. Sci., Vol. 243, 140, 1973.

31. Soifer, B.T., J.R. Houck and M. Harwit, "Rocket Infrared Observations of the Interplanetary Dust", Astrophys. J. (Letters), Vol. 168, L73, 1971.

32. Briotta, D.A., J.L. Pipher and J.R. Houck, Rocket Infrared Spectroscopy of the Zodiacal Dust Cloud, AFGL-TR-76-0236 (AD A034 054); D.A. Briotta, Ph.D. Thesis, Cornell University.

33. Sanford, S.A. and R.M. Walker, "Laboratory Infrared Transmission Spectra of Individual Interplanetary Dust Particles from 2.5 to 25 Micron", Astrophys. J., Vol. 291, 838, 1985.

34. Price, S.D., T.L. Murdock and L.P. Marcotte, "Infrared Observations of the Zodiacal Dust Cloud", Astron. J., Vol. 85, 1980.

35. Murdock, T.L., Infrared Emission from the Interplanetary Dust Cloud at Small Elongations, AFGL-TR-77-0280 (ADC 013 735), 1977.

36. Murdock, T.L., and S.D. Price, "Infrared Measurements of Zodiacal Light", Astron. J., Vol. 90, 375, 1985.

37. Hauser, M.G., F.C. Gillett, F.J. Low, N.T. Gautier, C.A. Beichman, G. Neugebauer, H.H. Aumann, N. Boggess, J.P. Emerson, J.R. Houck, B.T. Soifer and R.G. Walker, "IRAS Observations of the Diffuse Infrared Background", Astrophys. J. (Letters), Vol. 278, L15, 1984.

38. Hauser, M.G. and J.R. Houck, "The Zodiacal Background in the IRAS Data", Light on Dark Matter, ed. F.P. Israel, D. Reidel, 39, 1986.

39. Frazier, E.N., D.J. Boucher and G.F. Mueller, A Self-Consistent Model of the Zodiacal Light Radiance, Aerospace Report TOR-0086 (6432-01)-1.

40. Hong, S.S., and I.K. Um, "Inversion of the Zodiacal Infrared Brightness Integral", Astron. Astrophys., submitted.

41. Dumont, R., and A.C. Levasseur-Regourdd, "Heliocentric Dependences of Zodiacal Emission, Temperature and Albedo", Light on Dark Matter, ed. F.P. Israel, D. Reidel, 45, 1986.

42. Hauser, M.G., T.N. Gautier, J. Good and F.J. Low, "IRAS Observations of the Interplanetary Dust Emission", IAU Colloq. 85: Properties and Interactions of Interplanetary Dust, D. Reidel, 43, 1985.

43. Dermott, S.F., P.D. Nicholson and B. Wolven., "Preliminary Analysis of the IRAS Solar System Dust Data", Asteroids, Comets, Meteors II, ed. C-I. Lagerkvist and H. Rickman, Uppsala, in press.

44. Deul, E., Physical Modelling of Zodiacal Light, Seminar Notes Kapteyn Lab., 14 Feb, 1986.

45. Low, F.J., D.A. Beintema, T.N. Gautier, F.C. Gillett, C.A. Beichmann, E. Young, H.H. Aumann, N. Boggess, J.P. Emerson, H.J. Habing, M.G. Hauser, J.R. Houck, M. Rowan-Robinson, B.T. Soifer, R.G. Walker and P.R. Wesselius, "Infrared Cirrus: New Components of the Extended Infrared Emission", Astrophys. J. (Letters), Vol. 278, L19, 1984.

46. Gautier, T.N., M.G. Hauser and F.J. Low, "Parallax Measurements of the Zodiacal Dust Bands with the IRAS Survey", Bull. Amer. Ast. Soc., Vol. 16, 442, 1984.

47. Dermott, S.F., P.D. Nicholson, J.A. Burns and J.R. Houck, "An Analysis of IRAS' Solar System Dust Bands", IAU Colloq. 85: Properties and Interactions of Interplanetary Dust, D. Reidel, 395, 1985.

48. Sykes, M.V. and R. Greenberg, "The formation of the IRAS Zodiacal Dust Bands", Icarus, Vol. 65, 51, 1986.

49. Tedesco, E., private communication.

50. Rowan-Robinson, M., private communication.

51. Davies, J.K., S.F. Green, B.C. Stewart, A.J. Meadows and H.H. Aumann, "The IRAS fast-moving object search", Nature, Vol. 309, 315, 1984.

52. Sykes, M.V., L.A. Lebofsky, D.M. Hunten and F.J. Low, "The Discovery of Dust Trails in the Orbits of Periodic Comets", Science, Vol. 232, 1115, 1986.

53. Green, S.F., Ph.D. Thesis; quoted by Davies, J.K., "Are the IRAS-detected Apollo asteroids extinct comets?", Mon. Not. Sov. Ast. Soc., Vol. 221, 19p, 1986.

54. Sykes, M.V., private communication.

55. Singer, S.F., J.E. Stanley and P. Kessel, "The LDEF Interplanetary Dust Experiment", IAU Colloq. 85: Properties and Interactions of Interplanetary Dust, D. Reidel, 117, 1985.

56. Baker, P.L., and W.B. Burton, "Investigation of Low-Latitude Hydrogen Emission in Terms of a Two Component Interstellar Gas", Astrophys. J., Vol. 198, 281, 1975.

57. Sanders, D.B., N.Z. Scoville and P.M. Solomon, "Giant Clouds in the Galaxy II. Characteristics of Discrete Features", Astrophys. J., Vol. 289, 373, 1984.

58. Balley, J., "Interstellar Molecular Clouds", Science, Vol. 232, 185, 1986.

59. Solomon, P.M., B.D. Sanders and A.R. Rivolo, "The Massachusetts - Stony Brook Galactic Plane CO Survey: Disk and Spiral Arm Molecular Clouds", Astrophys. J. (Letters), Vol. 292, L19, 1985.

60. Harris, S., and M. Rowan-Robinson, "The Brightest Sources in the AFCRL Survey", Astron. Astrophys., Vol. 60, 405, 1977.

61. Gautier, T.N., "Observations of Infrared Cirrus", Light on Dark Matter, ed. F.P. Israel, D. Reidel, 49, 1986.

62. Armstrong, J.W., J.M. Cordes and B.J. Rickett, "Density power spectrum in the local interstellar medium", Nature, Vol. 291, 561, 1981.

63. Fleck, Jr., R.C., "A Note on Compressibility and Energy Cascade in Turbulent Molecular Clouds", Astrophys. J. (Letters), Vol. 272, L45, 1983.

64. O'Dell, C.R., "Turbulent Motion in Galactic H II Regions", Astrophys. J., Vol. 304, 767, 1986.

65. Sandage, A., "High-latitude reflection nebulosities illuminated by the galactic plane", Astron. J., Vol. 81, 955, 1976.

66. DeVries, C.P. and R.S. LePoole, "Comparison of optical appearance and infrared emission of some high latitude clouds", Astron. Astrophys., Vol. 145, L7, 1985.

67. Boulanger, F., B. Baud and G.D. van Albeda, "Warm dust in the neutral interstellar medium", Astron. Astrophys., Vol. 144, L9, 1985.

68. Weiland, J.L., L. Blitz, E. Dwek, M.G. Hauser, L. Magnani and L.J. Rickard, "Infrared Cirrus and High-Latitude Molecular Clouds", Astrophys. J. (Letters), Vol. 306, L101, 1986.

69. Savage, B.D. and J. Mathis, "Observed Properties of Interstellar Dust", Ann. Rev. Astron. Astrophys., Vol. 17, 73, 1979.

70. Marwit, M., J.R. Houck and G.J. Stacey, "Is IRAS cirrus cloud emission largely fine structure radiation", Nature, Vol. 319, 646, 1986.

71. Leene, A., "Warm dust in the R CrA molecular cloud", Astron. Astrophys., Vol. 154, 296, 1986.

72. Draine, B.T. and N. Anderson, "Temperature Fluctuation and Infrared Emission from Interstellar Grains", Astrophys. J., Vol. 292, 494, 1985.

73. Cox, P., E. Krugel and P.G. Mezger, "Principal heating sources of dust in the galactic disk", Astron. Astrophys., Vol. 155, 380, 1986.

74. Puget, J.L., A. Leger and F. Boulanger, "Contribution of large polycyclic aromatic molecules to the infra-red emission of the interstellar medium", Astron. Astrophys., Vol. 142, L19, 1985.

75. Leger, A., and J.L. Puget, "Identification of the "unidentified" IR emission features of interstellar dust", Astron. Astrophys., Vol. 137, L5, 1984.

76. Leger, A., and L. D'Hendecourt, "Are aromatic hydrocarbons the carriers of the diffuse bands in the visible", Astron. Astrophys., Vol. 146, 81, 1985.

77. Crawford, M.K., A.G.G. Tielens and L.A. Allamandola, "Ionized Polycyclic Aromatic Hydrocarbons and the Diffuse Interstellar Bands", Astrophys. J. (Letters), Vol. 293, L45, 1985.

78. Duley, W.W., and D.A. Williams, "PAH Molecules and carbon dust in interstellar cloud", Mon. Not. Roy. Ast. Soc., Vol. 219, 859, 1986.

79. Hayakawa, S., T. Matsumoto, H. Murakami, K. Uyama, J.A. Thomas and T. Yamagami, "Distribution of near infrared sources in the galactic disk", Astron. Astrophys., Vol. 100, 116, 1981.

80. Little, S.J. and S.D. Price, "Infrared Mapping of the Galactic Plane. IV. The Galactic Center", Astron. J., Vol. 90, 1812, 1986.

81. Hayakawa, S., K. Noguchi and K. Uyama, "Near Infrared Multicolor Observations of the Diffuse Galactic Emission", Publ. Ast. Soc. Jap., 1982.

82. Willner, S.P., B.T. Soifer, R.W., Russell, R.R. Joyce and F.C. Gillett, "2 to 8 Micron Spectro-photometry of M82", Astrophys. J. (Letters), Vol. 217, L121, 1977.

83. Houck, J.R., W.J. Forrest and J.M. McCarthy, "Medium-Resolution Spectra of M82 and NGC 1068", Astrophys. J. (Letters), Vol. 242, L65, 1980.

E AND

WIS6

DTIC